



**HAL**  
open science

# GFRP MECHANICAL BEHAVIOUR INDUCED BY A MESOSCOPIC SHAPING DEFECT

Anwar Shanwan, C. Cruanes, Samir Allaoui, Stéphane Méo, Marie-Pierre Deffarges, F. Lacroix, G. Hivet

► **To cite this version:**

Anwar Shanwan, C. Cruanes, Samir Allaoui, Stéphane Méo, Marie-Pierre Deffarges, et al.. GFRP MECHANICAL BEHAVIOUR INDUCED BY A MESOSCOPIC SHAPING DEFECT. 21st International Conference on Composite Materials, Aug 2017, Xi'an, China. hal-02481013

**HAL Id: hal-02481013**

**<https://hal.science/hal-02481013>**

Submitted on 17 Feb 2020

**HAL** is a multi-disciplinary open access archive for the deposit and dissemination of scientific research documents, whether they are published or not. The documents may come from teaching and research institutions in France or abroad, or from public or private research centers.

L'archive ouverte pluridisciplinaire **HAL**, est destinée au dépôt et à la diffusion de documents scientifiques de niveau recherche, publiés ou non, émanant des établissements d'enseignement et de recherche français ou étrangers, des laboratoires publics ou privés.

# GFRP MECHANICAL BEHAVIOUR INDUCED BY A MESOSCOPIC SHAPING DEFECT

A. Shanwan<sup>2</sup>, C. Cruanes<sup>1</sup>, S. Allaoui<sup>2</sup>, S. Méo<sup>1</sup>, M.-P. Deffarges<sup>1</sup>, F. Lacroix<sup>1</sup>, G. Hivet<sup>2</sup>

<sup>1</sup> LMR laboratory, EA 2640, Tours university, 7 avenue Marcel Dassault 37000 Tours, France.  
[christophe.cruanes@univ-tours.fr](mailto:christophe.cruanes@univ-tours.fr), [florian.lacroix@univ-tours.fr](mailto:florian.lacroix@univ-tours.fr); [stephane.meo@univ-orleans.fr](mailto:stephane.meo@univ-orleans.fr)

<sup>2</sup> PRISME laboratory, Orléans university, 8 rue Leonard de Vinci, 45072 Orleans Cedex 2, France.  
[samir.allaoui@univ-orleans.fr](mailto:samir.allaoui@univ-orleans.fr), [anwar.shanwan@univ-orleans.fr](mailto:anwar.shanwan@univ-orleans.fr); [gilles.hivet@univ-orleans.fr](mailto:gilles.hivet@univ-orleans.fr)

**Keywords:** forming process, defects, fatigue, induced behaviour

## ABSTRACT

The aim of this study is to evaluate the effect of the “buckles” mesoscopic defects on the composites mechanical properties. For this purpose, an analysis was made on the kinematics involved during the appearance of these defects on complex shapes. Then, a device and a protocol were developed in order to realize calibrated specimens. “Buckles” defects have been generated on glass plane weave fabric layers taking care to reproduce the amplitudes observed on a complex preforms. Composites plates with seven stacked layers were then injected and specimens were cut in different areas before mechanically testing them under static and fatigue tensile tests. The results showed that the “buckles” defects have an effect on the static and fatigue behavior of the specimens with defects. The measured strain using DIC method showed the presence of damage in the specimen’s areas with defects, which induced a loss of rigidity and a decrease of the ultimate stress. The specimen with transverse defects showed a more significant loss of mechanical performances.

## 1 INTRODUCTION

The composites materials are widely used in the industry thanks to their very good mechanical characteristics for a lower mass than metal alloys. To manufacture these composites, especially when dealing with complex geometries, parts LCM processes are among the best candidates. However, these processes might induce defects like during textiles forming.

Those defects can be divided in two groups: macroscopic and mesoscopic. Macroscopic defects (wrinkles), appearing at the fabric scale, are the most common and studied in the literature. Wrinkles appearance highly depends on the fabric behavior and boundary conditions and can lead to bad quality of the parts coupled to a significant decrease of the composite performance [1-5]. The second kind of defects, the mesoscopic defects, appears at the yarn level. Among those, there may be mentioned fibers and/or yarn breakage, “buckles”, “weave pattern heterogeneity”, “yarn waviness”, etc... [3, 6-8]. There are few studies treating of these mesoscopic defects and their effect the induced behavior of the composite despite the fact that they are more recurring during complex preforms shaping [3, 4].

The aim of this study is to evaluate the effect of the “buckles” defects, which is an out of plane mesoscopic defect (figure 1), on the induced mechanical behavior of a GFRP composite. First, “buckles” have been generated on glass plane weave dry fabric layers using a specific bench designed and developed for this purpose. The plies with calibrated defects have been produced taking care to reproduce the amplitudes observed on a complex preform (see figure 1) used in a precedent study [3]. Plates, of seven stacked layers, were then performed by injecting epoxy resin using RTM process.

Plates without defects were also performed to be used as a reference. Specimens were cut in the transverse and longitudinal direction of the composite plates to perform static and fatigue tensile tests.

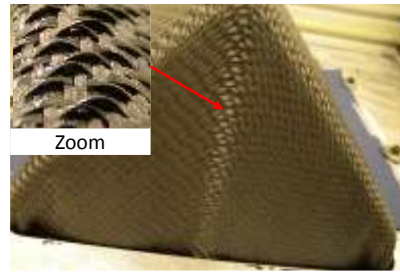


Figure 1: “Buckles” mesoscopic defects observed on double curved shape with carbon fabric

## 2 MATERIAL AND METHODS

### 2.1 Mesoscopic defects

This study deals with the “buckle” mesoscopic defect that appears at the yarn level. This defect appears when the yarns are submitted to buckling out of plane of the fabric (Figure 2). This leads locally to a significant overthickness that can achieve several times the initial thickness of the fabric. For example, for the case of only one layer of G1151 interlock, this overthickness reaches 5 mm, while the fabric thickness is only about 0.62 mm. Therefore, this defect may be a cause for disposal of composite parts after their manufacturing for geometric non-compliance. In addition, this defect may have an effect on the behavior of the obtained composite hence the need to evaluate its criticality and understand the involved mechanisms in order to develop shaping strategies for achieving healthy preforms. To achieve this purpose, this study proposes to evaluate the effect of this defect by performing mechanical tests on calibrated specimens.



Figure 2: “buckles” mesoscopic defect.

### 2.2 Material used

The material used in this study is a glass fiber reinforced polymer. VARTM process was used to produce composite plates. The fabric used is a balanced glass plain weave produced by Chomarat Company. It is denoted G-WEAVE 600P and has the following properties: a real weight of  $600 \text{ g / m}^2 \pm 5\%$ , thickness of 0.55 mm, warp and weft yarns count of 600 Tex. Thermosets epoxy resin LY564 ARALDITE with a suitable hardener 3487 ARADUR was used to inject staking performed according to the protocol described below.

### 2.3 Specimens preparation

To realize these specimens, the kinematics of the apparition of the “buckles” was identified on preforming tests done on tetrahedron punch (Figure 3). Figure 3 shows that this defect appears on a

tape with a width of about 3cm located at the center of the face. This area is delimited with two zones where the shear angles are in the same order of magnitude (here  $24^\circ$ ), but that occur in two opposite directions: clockwise and counterclockwise [3, 4]. On the area with defects, one network of yarns (here in blue) are bended, while the yarns of the other network (in red) remain straight and are submitted to a large tension due to severe geometry of the top of the punch which is a triple point. We can conclude that the triple point apply a tension on the straight yarns that carry with them the transverse yarns (due to the fabric cohesion) inducing the two shear areas and the bending of the yarns in blue and consequently their out of plane buckling.

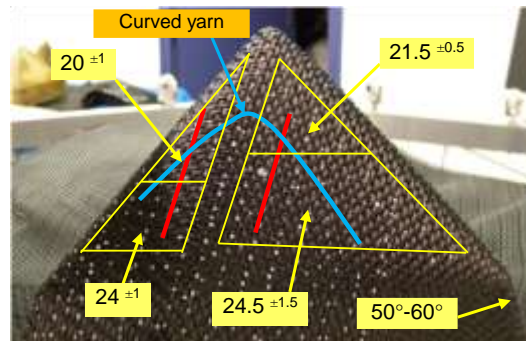


Figure 3: Tetrahedron preform realized with interlock dry fabric.

A specific bench was designed and developed in order to study the “buckles” defects and produce calibrated specimens. The device consists of four axes that can be controlled separately in force or displacement. Preliminary work focusing especially on the boundary conditions was carried out during the commissioning of the device.

To produce specimens for the study, two kind of composites plates were manufactured: plates with defect and plates with calibrated defects. In order to produce plates without defects (healthy), the reinforcement was cut into square samples of  $250 \times 250 \text{ mm}^2$ . The dimensions were selected to fit with the mold size. For plates with buckles defect, the reinforcement was cut into square samples of  $500 \times 500 \text{ mm}^2$ . Then, the sample was placed on the bench and the generation of the “buckle” defects was obtained by applying the optimal kinematic and boundary conditions. After reaching the needed amplitude of defects, the sample is kept fixed and a fixing agent is sprayed on the surface of the fabric sample. When the sprayed layer becomes dry, the calibrated sample can be removed and then cut into a square shape of  $250 \times 250 \text{ mm}^2$ . Several plies with calibrated defects have been produced according to this protocol.

After producing plies of fabrics (with and without defects), staking of 7 plies oriented in the same orientation ( $0^\circ$ ) was performed and placed in the VARTM mold. Then, the epoxy matrix is injected and the mold transferred into a preheated oven at  $100^\circ\text{C}$ . After 3 hours, the mold was removed and kept cooling down at ambient temperature for 6 hours. All precautions have been taken in order to have plates without porosities. The final thickness of the obtained composite plates is about 2.5 mm.

Test specimens were subsequently cut on the injected composite plates to test them mechanically. These specimens were divided into three batches according to their origin. The first group is that of healthy specimens cut on the reference plates. The second batch, denoted A, was obtained on the sheared regions of the plates with calibrated defects ((Figure 4). The third group, noted B, consists of specimens cut from the area with the «buckles» defects ((Figure 4). Subsequently uniaxial tensile tests with optical measurements were carried out on these samples and the results are presented in the next section.

After producing composite plates, specimens for mechanical tests were cut out using waterjet cutting. Those samples were all designed following the ISO 527-4 1B allowing the use of lower capacity load cells and the localization of the damage in a central area of the sample, away from the clamps.

Three configuration of samples were produced. The first one is specimens without defects (healthy specimens) that will be considered as reference in the study. As the fabric is balanced, only one

configuration of the healthy specimen is considered without differentiating the two direction (weft and warp) of the plates. This assumption has been validated with DMA measurements performed on the GFRP which showed that the mechanical characteristics were similar along the warp and weft orientations. These specimens will be noted “ND” which means no defects specimens.

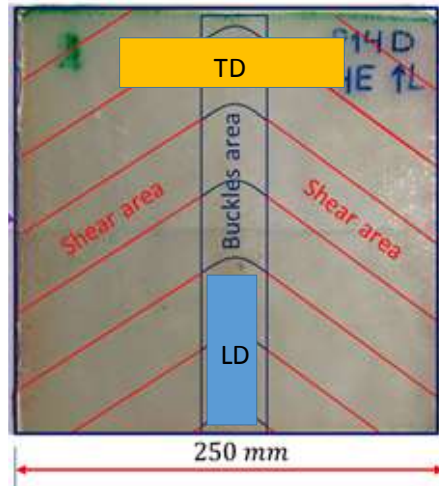


Figure 4: Example of composite plate with “buckle” defects

For the specimens with defects, two configuration were considered: transverse direction (noted TD) and longitudinal direction (noted LD). Longitudinal defect samples, or « LD », cut along the area of the plates containing the calibrated buckle defects. The defect is placed on the central axis along the sample (figure 4). Transverse defect samples, or « TD », cut in the transverse direction of the plates with calibrated defects. The buckles are oriented at 90° with respect to the central axis of the sample (figure 4) and are present only locally in an area on the center of the sample.

## 2.4 Experimental tests

In order to investigate the effect of the buckles mesoscopic defects and its orientation on the mechanical behavior of the GFRP, static and fatigue tests were performed. They were both conducted on an Instron 8872 servo-hydraulic fatigue testing machine at room temperature. The static tests were displacement controlled at 2mm/min. The loading cells used were with a capacity of 25kN for the ND and LD samples and 5kN for the TD. The sampling used was 100Hz. The fatigue tests were carried out using the same machine and loading cells. The tests were stress controlled, uniaxial, at 5Hz and with a 0.1 load ratio (defined as the ratio between the lowest and highest stress undergone by the sample during a cycle  $\sigma_{min}/\sigma_{max}$ ) to ensure that the samples would not undergo buckling.

Table1 shows the solicitations investigated for the three types of samples. The tests were carried out until failure of the sample and were chosen to cover from 50% of the ultimate stress  $\sigma_u$ , measured during the static test, to 25% of  $\sigma_u$  for the ND samples. For the two other types of samples, the tests started also at 50% of  $\sigma_u$  and then the maximum strain has been steadily decreased based on the fatigue life of previous solicitations. The lower solicitation for which a failure of the sample occurred was at 40% of  $\sigma_u$  for the TD and 25% of  $\sigma_u$  for the LD.

Digital Image Correlation (DIC) device was used to measure the strain field during tests. A CCD camera (2448x2048 pixels) and the ARAMIS acquisition software have been used. The samples were prepared by firstly a layer of white paint and secondly a random pattern of dots with black paint in order to get a contrasted surface in front of the cameras. Firstly, the strain was directly measured by

the fatigue machine and then corrected with DIC measurements every 20 minutes (or 10 minutes for the shorter tests) to take into account the compliance of the machine.

	Maximum effort $F_{max}$ (kN)	Maximum global stress $\sigma_{max}$ (MPa)	Maximum global normalized stress $\frac{\sigma_{max}}{\sigma_{ult}}$	Fatigue life $N_f$ (cycles)
LD samples	5	193,80	0,50	1250
	3	111,11	0,30	9763
	2,75	104,56	0,28	15734
	2,5	88,34	0,25	30713
	2,25	82,42	0,23	55402
	2	73,53	0,20	302000
	1,8	70,87	0,18	1035560
	1,6	62,99	0,16	20000
TD samples	1,25	46,30	0,13	4700000
	0,25	9,96	0,31	>11680000
	0,375	14,82	0,46	77400
	0,375	14,94	0,47	>2900000
	0,375	14,76	0,46	103539
	0,375	14,76	0,46	1029370
	0,375	15,12	0,47	954000
	0,4	16,13	0,51	222000
	0,4	15,59	0,49	43200
	0,4	15,94	0,50	52300
	0,4	16,13	0,51	895000
	0,4	15,33	0,48	13375
	0,45	18,07	0,57	95221
	0,45	17,51	0,55	12000
	0,45	18,99	0,60	25000
	0,45	18,07	0,57	546000
	0,5	20,41	0,64	139200
	0,5	20,33	0,64	18038
0,5	19,46	0,61	12000	
0,5	20,62	0,65	13700	
0,5	20,16	0,63	17800	
ND samples	6	220,59	0,49	8000
	5	190,84	0,42	14000
	4	151,52	0,34	86000
	4,5	163,64	0,36	41027
	4,5	163,64	0,36	48000
	3,5	132,08	0,29	277168
	3,35	127,38	0,28	1693820
	3,25	116,91	0,26	2077000
3	112,78	0,25	3279000	

Table 1 – List of the solicitations investigated in fatigue depending of the type of defect and the fatigue life associated. If the latter is in red, it means that the test was stopped before the failure.

### 3 RESULTS AND DISCUSSION

Figure 5 illustrates an example of the stress-strain curves of the three configuration of samples (ND, LD and TD). We observe that the ND and LD samples have close evolutions, moduli and ultimate stresses. For the TD specimens, we observe a significant decrease in the mechanical behavior, elastic and failure characteristics. Consequently, the TD sample differs greatly with much lower mechanical characteristics. This is the consequence of the presence defect and the fact that there are no more yarns oriented in the loading direction as these yarns are those who are submitted to out of plane buckling and as a consequence they rotate on the areas adjacent to the defects. The oriented yarns have an effect on the rigidity and the failure characteristics while the “buckles” defects contribute to the early failure of the specimens. This effect can be correlated to the strain distribution measured with the DIC where we can observe a high strains, which are rather damage presence and propagation, located in the central part of the sample where the buckles are present (figure 6).

The slight decrease in the ultimate decrease of the LD specimen can be attributed to the mesoscopic defect, which causes damage initiation and promotes its propagation. This can be seen in the strain

distribution of the specimen (figure 6) where the local strains measured are very high in the area where there is buckles. These high strains follow the direction of the buckled yarns.

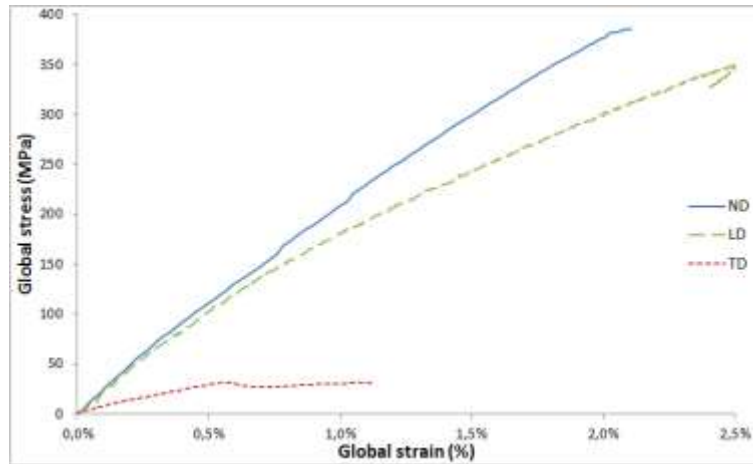


Figure 5 – Evolution of the stress versus the strain for the ND, LD and TD samples (1 test by curve)

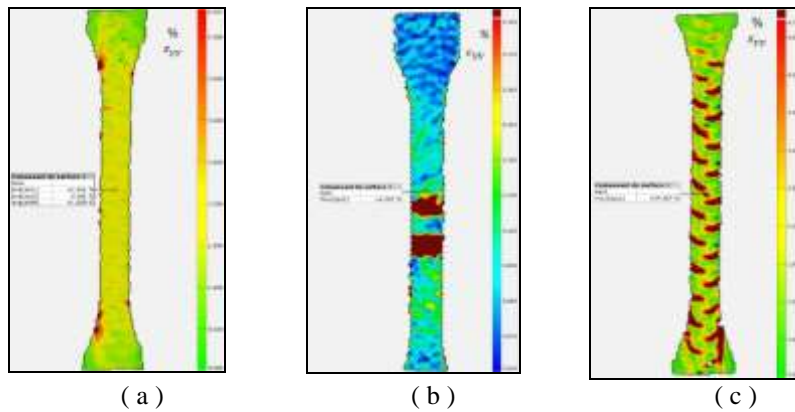


Figure 6: Strains distribution on samples during static tests: (a) healthy sample (b) sample with transverse defects (c) sample with longitudinal defects).

The Wohler curves obtained with fatigue tests for the three configuration of samples are presented on figure 7. The ND samples showed an evolution with a limit between LCF and HCF around 29% of the ultimate stress, at a stress of 132MPa. The stiffness decreased during fatigue tests. Two phases can be identified: a slow decrease followed by a faster one until the failure of the sample. The intensity of the first phase depends on the sollicitation: the stronger the maximum stress, the stiffer the slope. The reason for this first slow decrease is that the pattern followed by the yarns (taffeta) generates some local plasticization, implying that the matrix will creep. Then, at some point during the test, cracks appeared and propagated, accelerating the decrease of the stiffness [9-10].

The fatigue characteristics of the LD samples are lower than ND with a LCF/HCF limit between 20% and 22% of the ultimate stress, at a stress around 78MPa. The TD samples were expected to have the lowest fatigue characteristics among the three types of sample given the static tests. The limit between low and high cycle fatigue is close to 45% of the ultimate stress, at a stress of 14MPa. The areas of maximum strain are in the neighborhood of the defect, which is the same as in static.

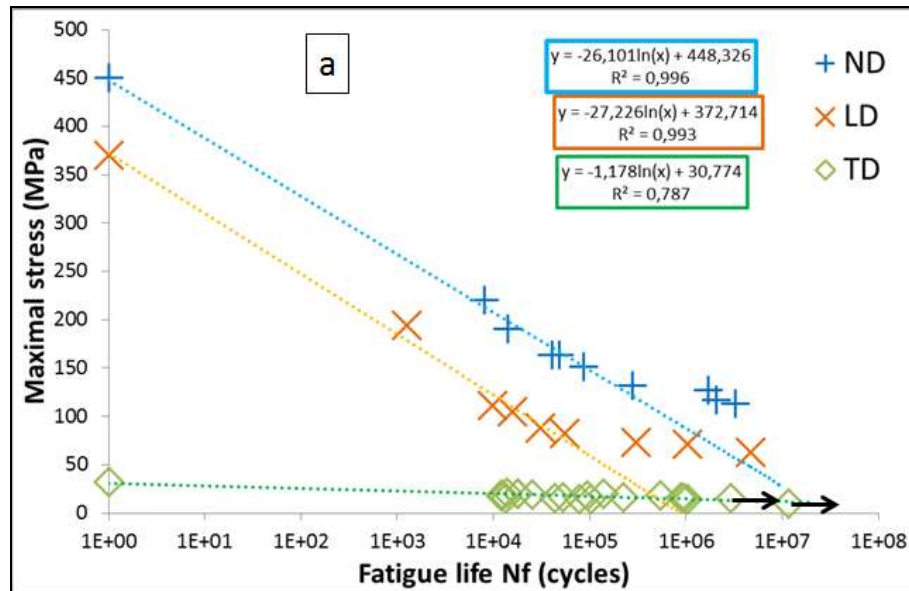


Figure 7 – Wöhler curve for each sample in a maximum stress/fatigue life chart. The dotted lines represent the fatigue behavior during the LCF phase.

#### 4 CONCLUSION

The aim of this work is to contribute to the understanding of the effect of “buckles” mesoscopic defects that are recurrent when dealing with preforming of complex shapes. To achieve this aim, a device was designed and built in order to produce calibrated specimens with calibrated defects. After validating the device, a protocol was established and specimens were realized with VARTM process.

The results of uniaxial tensile tests, under static and fatigue loading, showed that the “buckles” defects have major effect on the GFRP mechanical behavior. The results revealed that both defect orientations (transverse and longitudinal) have a significant effect on the fatigue life and on the strain field distribution. Specimens with defects in the transverse direction are the most crippling condition but the longitudinal direction configuration was also very affected by the presence of the mesoscopic defects. Those observations lead to conclude that this mesoscopic out of plane defect has a major negative influence on the fatigue life of such a composite and must be considered when designing technical parts.

#### ACKNOWLEDGMENT

The authors wish to thank Centre-Val-de-Loire Region for its financial support in the project IDDEFORM. They also would thank the team from the CERMEL and more particularly Mathieu Venin for his precious help.

#### REFERENCES

- [1] Boisse P., Hamila N., Vidal-Sallé E., Dumont F. Simulation of wrinkling during textile composite reinforcement forming. Influence of tensile, in-plane shear and bending stiffness. *Compos. Sci. Tech.*, 2011; 71:683-692.
- [2] Wilems A., Lomov S., Verpoest I., Vandepitte D., Harrison P., Yu W. Forming simulation of a thermoplastic commingled woven textile on a double dome. *Int.Jour. of Mat. Form.*, 2008; 1:965-968.

- [3] S. Allaoui, G. Hivet, D. Soulat, A. Wendling, P. Ouagne, S. Chatel, Experimental preforming of highly double curved shapes with a case corner using an interlock reinforcement, *International Journal of Material Forming*, 7(2), 2014, pp.155-165.
- [4] Allaoui S., Boisse P., Chatel S., Hamila S., Hivet G., Soulat D., Vidal-Salle E. Experimental and numerical analyses of textile reinforcement forming of a tetrahedral shape. *Composites: Part A*, 2011; 42:612-622
- [5] Hallander P., Akermo M., Mattei C., Petersson M., Nyman T. An experimental study of mechanisms behind wrinkle development during forming of composite laminates. *Composites: Part A*, 2013; 50:54-64.
- [6] Potter K., Khan B., Wisnom M., Bell T., Stevens J. Variability, fibre waviness and misalignment in the determination of the properties of composite materials and structures. *Composites: Part A*, 2008; 39:1343-1354.
- [7] Lightfoot J.S., Wisnom M., Potter K. Defects in woven preforms: formation mechanisms and the effects of laminate design and layup protocol. *Composites: Part A*, 2013; 51:99-107.
- [8] Härtel F., Middendorf P. Process parameters studies and comparison of different preform processes with NCF material. In proceeding of ICCM-19. Montreal, July, 2013.
- [9] Demers C.E. Tension-tension axial fatigue of E-glass fiber-reinforced polymeric composites: tensile fatigue modulus. *Constr. Build. Mat.*, 1998; 12(1):51-58
- [10] Montesano J., Fawaz Z., Bougherara H. Non –destructive assessment of the fatigue strength and damage progression of satin woven fiber reinforced polymer matrix composites. *Composites: Part B*, 2015; 71:122-130